Cracking the DM code at the LHC

Wonsang Cho (University of Florida)

in collaboration with
Doojin Kim, Konstantin Matchev and Myeonghun Park

PHENO 2012
5. 8. 2012

UF UNIVERSITY of FLORIDA

General decay chains with N_v-visibles and N_x-invisibles

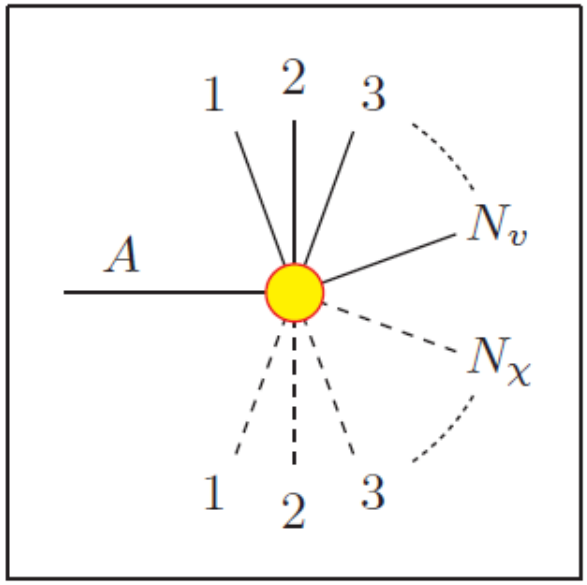

Number of possible decay topologies ?

- **Trivial caterpillars**

- **Non-trivial caterpillars with sub-cater.**

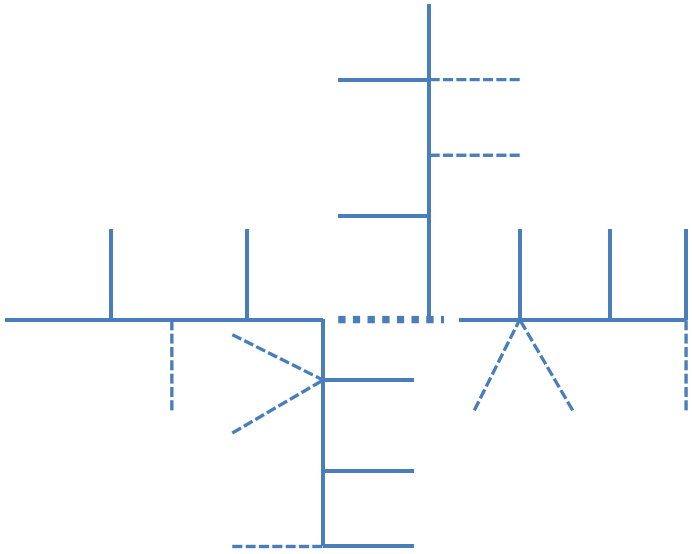

Table (1) Number of possible caterpillars

$N_v(\Downarrow), N_\chi(\Rightarrow)$	1	2	3	4	5
1	1	2	4	8	16
2	2	6+1	16+4	40+15	96+46
3	4	16+4	52+26	152+120	416+452
4	8	40+15	152+120	504+657	1536+2774
5	16	96+46	416+452	1536+2774	5136

- **We concentrate on M_{vis}** for surveying on the perspectives of

  1) **Discrimination of decay topology**
  2) **Mass measurement**

- **M_{vis}** is the most simplest observable, minimizing the ambiguities from

  a) **Combinatorics**
  b) **Energy of the mother particle**

  → The shape of **M_T** (transverse mass) constructed with visible + invisible information altogether, changes with the energy of the mother particle

- So, we study on **$d\Gamma/dM_{visible}$**, **Peak/Endpoint** vs **Peak structure**, checking the possibility of resolving 1) and 2) in a pure kinematic basis.

*) References on topology discrimination/reducing combinatorics errors:

K. Agashe, D. Kim, M. Toharia and D. G. E. Walker, PRD (2010); K. Agashe, D. Kim, D.G.E. Walker and L. Zhu, PRD (2011); Y. Bai and H. –C. Cheng, JHEP (2011); G.F. Giudice, B. Gripaios and R. Mahbubani, arXiv:1108.1800; A. Rajaraman and F. Yu PLB (2011); P. Baringer, K. Kong, M. McCaskey and D. Noonan, JHEP (2011); K. Choi, D. Guadagnoli and C. B. Park, JHEP (2011); M. M. Nojiri, Y. Shimizu, S. Okada and K. Kawagoe, JHEP (2008); D. Curtain, PRD (2012); K. Dienes, S. Su and B. Thomas, arXiv:1204.4183 .....

The case of $N_v = 2$ with $N_\chi = 1$, 2, & 3(partly)

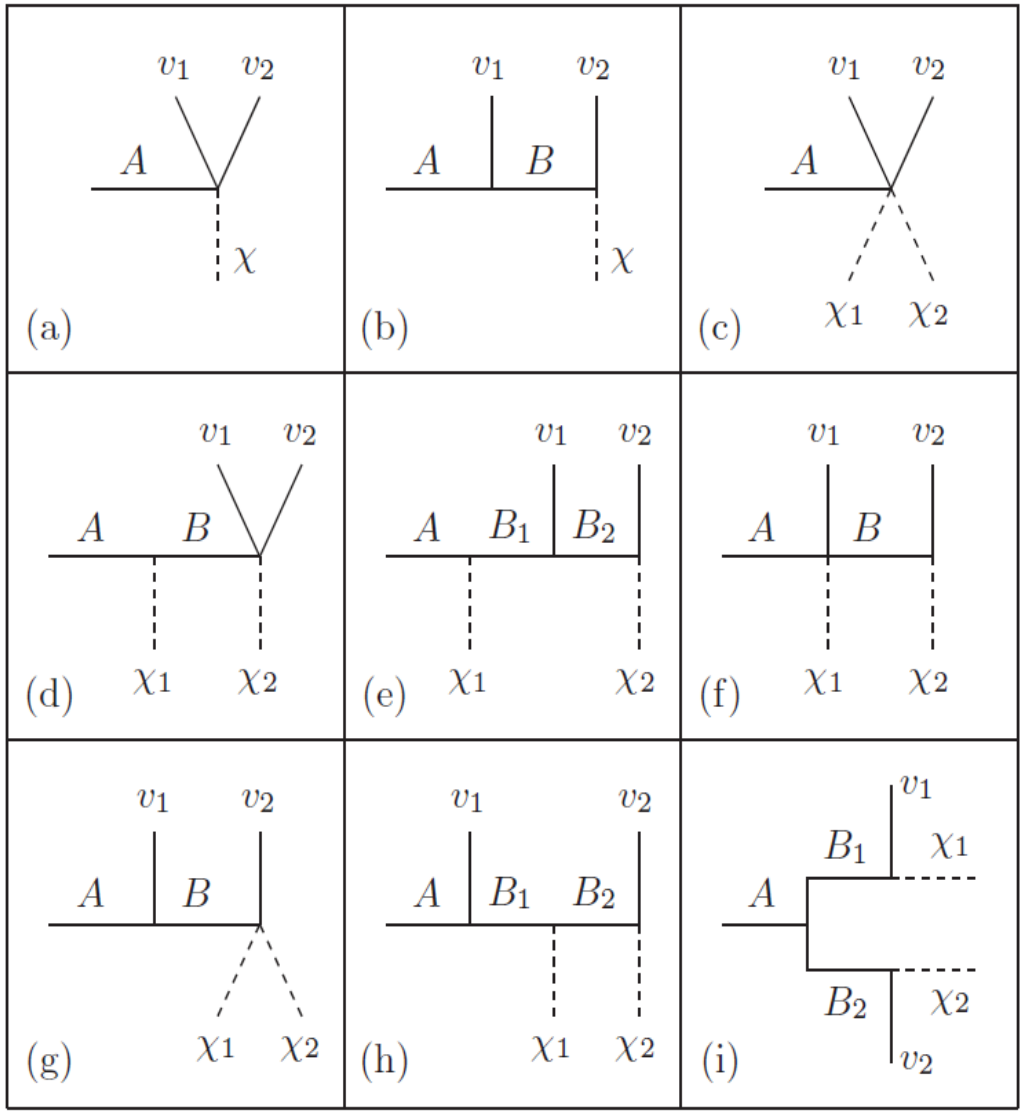

Nx=1 : (a) (b)
Nx=2 : (c) ~ (i)
Nx=3 : (j)

BETWEEN the two visibles :

- Including N(≥3) body decay vertices
  → (a,d) (c) (f) (g)

- Connected through only 2-body decay vertices
  → (b,e) (h) (j) (i)

+

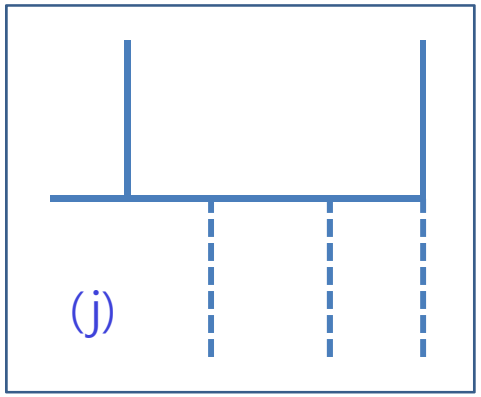

Topologies including N(≥3) body decay chains (``The rubber arms")

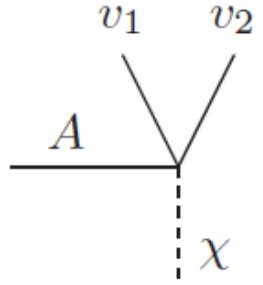

$$f(m; M_A, M_\chi) \sim m\,\lambda^{1/2}\left(m^2, M_A^2, M_\chi^2\right)$$

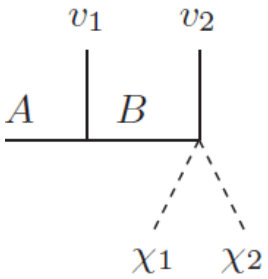

$$f(m) \sim m \int_{(M_{\chi_1}+M_{\chi_2})^2}^{M_B^2\left(1-\frac{m^2}{M_A^2-M_B^2}\right)} \frac{\sqrt{\lambda(s, M_{\chi_1}^2, M_{\chi_1}^2)}}{s} ds$$

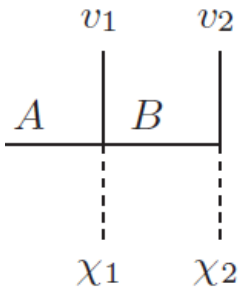

$$f(m) \sim m \int_{M_B^2\left(1+\frac{m^2}{M_B^2-M_{\chi_2}^2}\right)}^{(M_A-M_{\chi_1})^2} \frac{\sqrt{\lambda(s, M_A^2, M_{\chi_1}^2)}}{s} ds$$

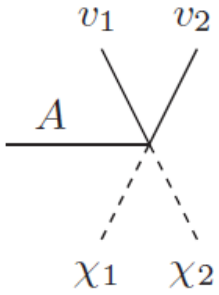

$$f(m) \sim m \int_{(M_{\chi_1}+M_{\chi_2})^2}^{(M_A-m)^2} \frac{\sqrt{\lambda(M_A^2, m^2, s)\lambda(s, M_{\chi_1}^2, M_{\chi_1}^2)}}{s} ds$$

- The length of the visible momenta can be stretched in the mother rest frame.
- Span phase space smoothly.

→ No cusp.

- Bunch of λ-functions.

Topologies with only 2 body decay vertices (``The robotic arms") → CUSP/Partitioning points

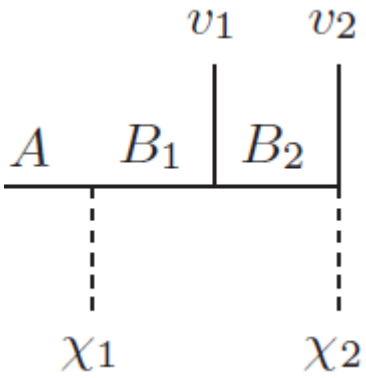

Triangle :
N_{INT} =1

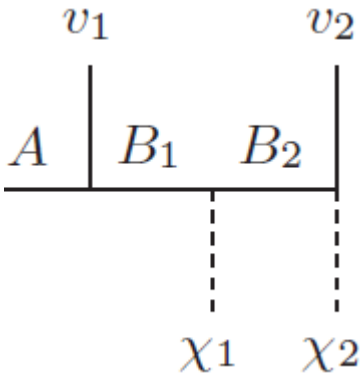

DM sandwiches[1]
N_{INT} =2

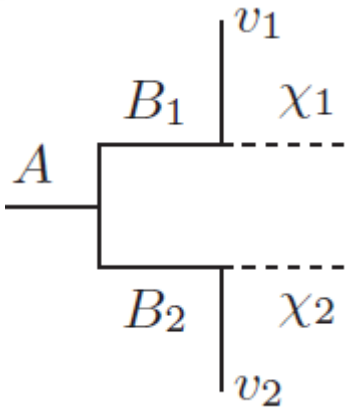

Antler[2]
N_{INT} =2

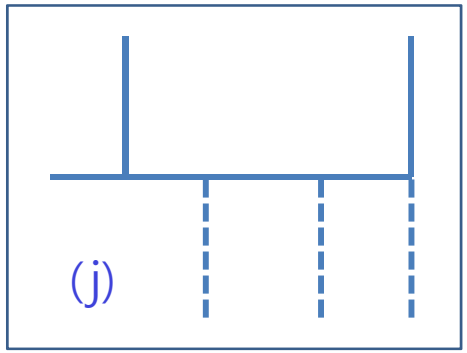

Double DM sandwich
N_{INT} =3

- The length of visible momentum fixed in mother's rest frame. Just spanning mother mass shell, like as robotic arms.
- Depending on the number of the intermediate particle and mass spectrum, they have several partitioning points, eventually a CUSP peak appears among them.

- The shape of the distributions in the initial lower range up to 1st separation point is always linear, regardless of mass spectrums and N_{INT}
- The Existence of CUSP depends of mass spectrum[2]

[1] K. Agashe, D. Kim, M. Toharia and D. G. E. Walker, PRD (2010);
[2] T. Han, I.-W. Kim and J. Song, PLB (2010)

Ex) Double DM sandwich

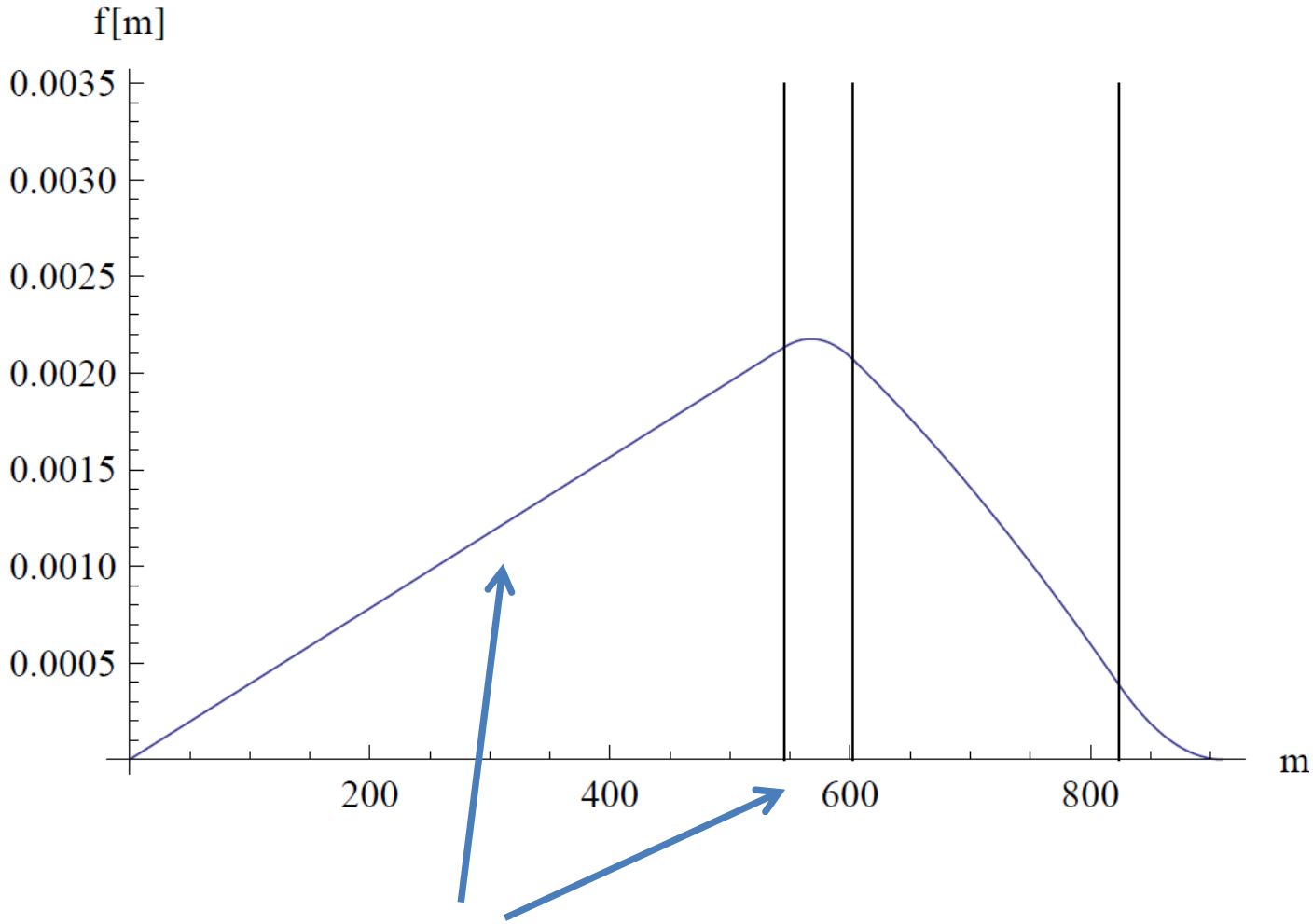

- Three partitioning points
- Linear for the 1st section

Peak-matched/normalized distributions, minimizing χ^2 to the reference ``Antler" distribution$^{2(\text{magenta})}$ in the whole range.

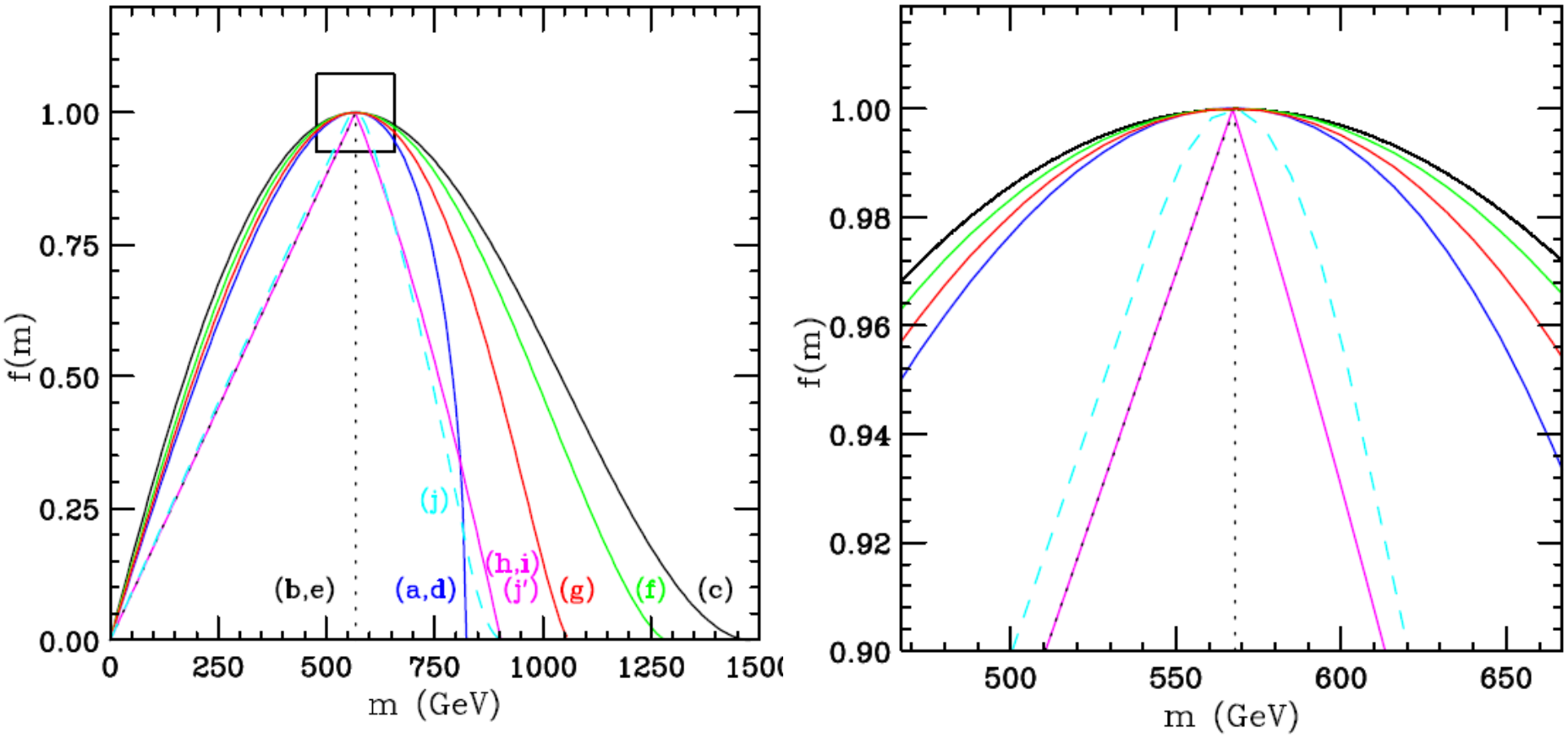

Peak-matched unit normalized distributions, minimizing χ^2 to the reference ``Antler" distribution

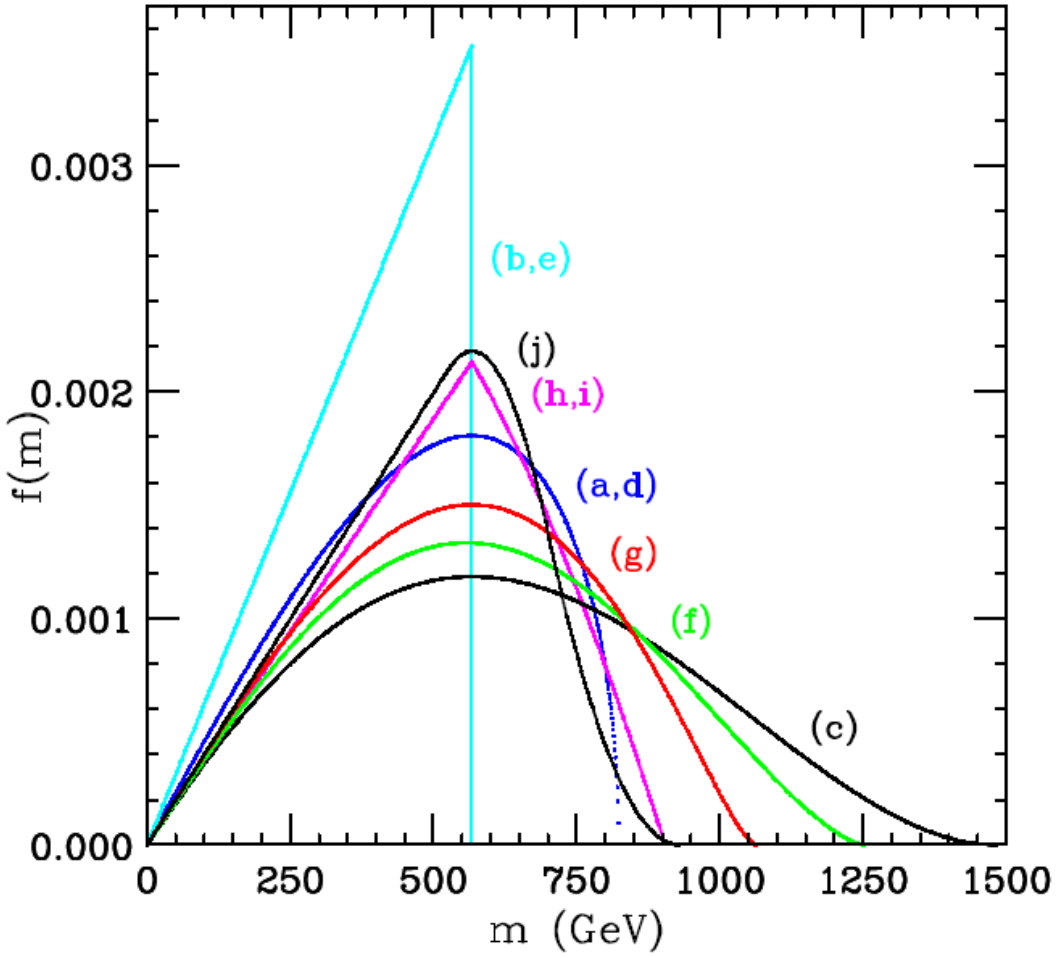

Topology Disambiguation Diagram (P/E vs R_n)

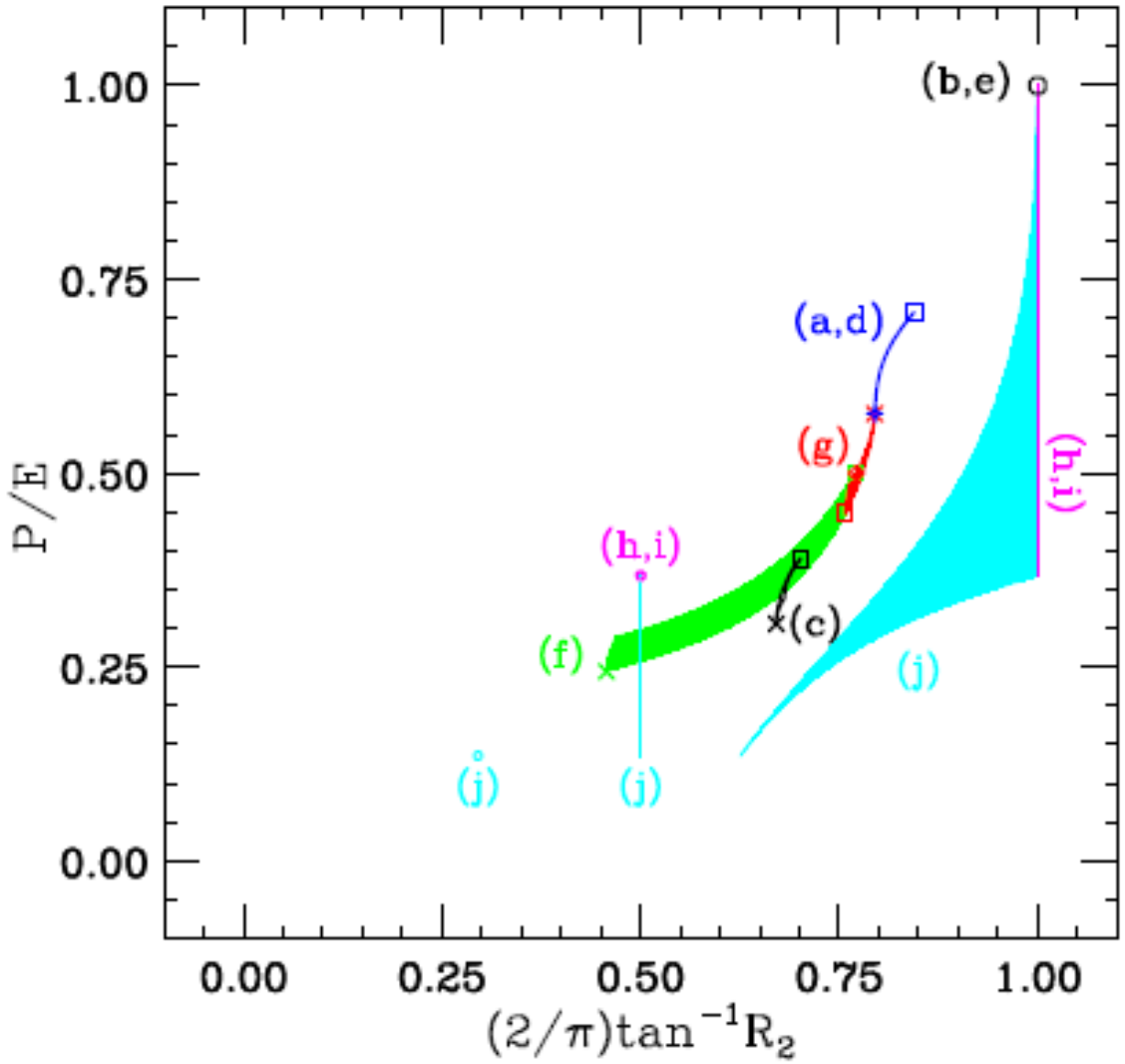

- P = peak
- E = endpoint
- $R_n = -\frac{m^n}{f(m)}\frac{d^n f(m)}{dm^n}$ $at\ m=P$

Observations & Strategy for topology discrimination

1) Critical difference between **the rubber arms** and **the pure robotic arms** :

→ Regardless of the mass spectrum, the pure robotic arms always have **linear** distributions up to 1st separation(cusp) point, which show large differences from the others of the rubber arms.

→ Large portion of the numbers in the caterpillar table can be removed.

2) **Even among the rubber arms, are they quite well-separated in their own ranges in the `Disambiguation plot' - P/E vs R_2**

→ Even though the R_2 is not likely to be measured precisely, a small difference in R_2 can result in large difference in the whole region of distributions, due to the strong correlations between P/E and R_2.

→ Then, **given a measured peak position of a reference dist.,** check the error bands of the minimized χ^2 values of the peak-matched distributions from the different topologies, w.r.t the reference distribution.

Minimized χ^2 – error band of each topology within the peak-matched mass parameter spaces

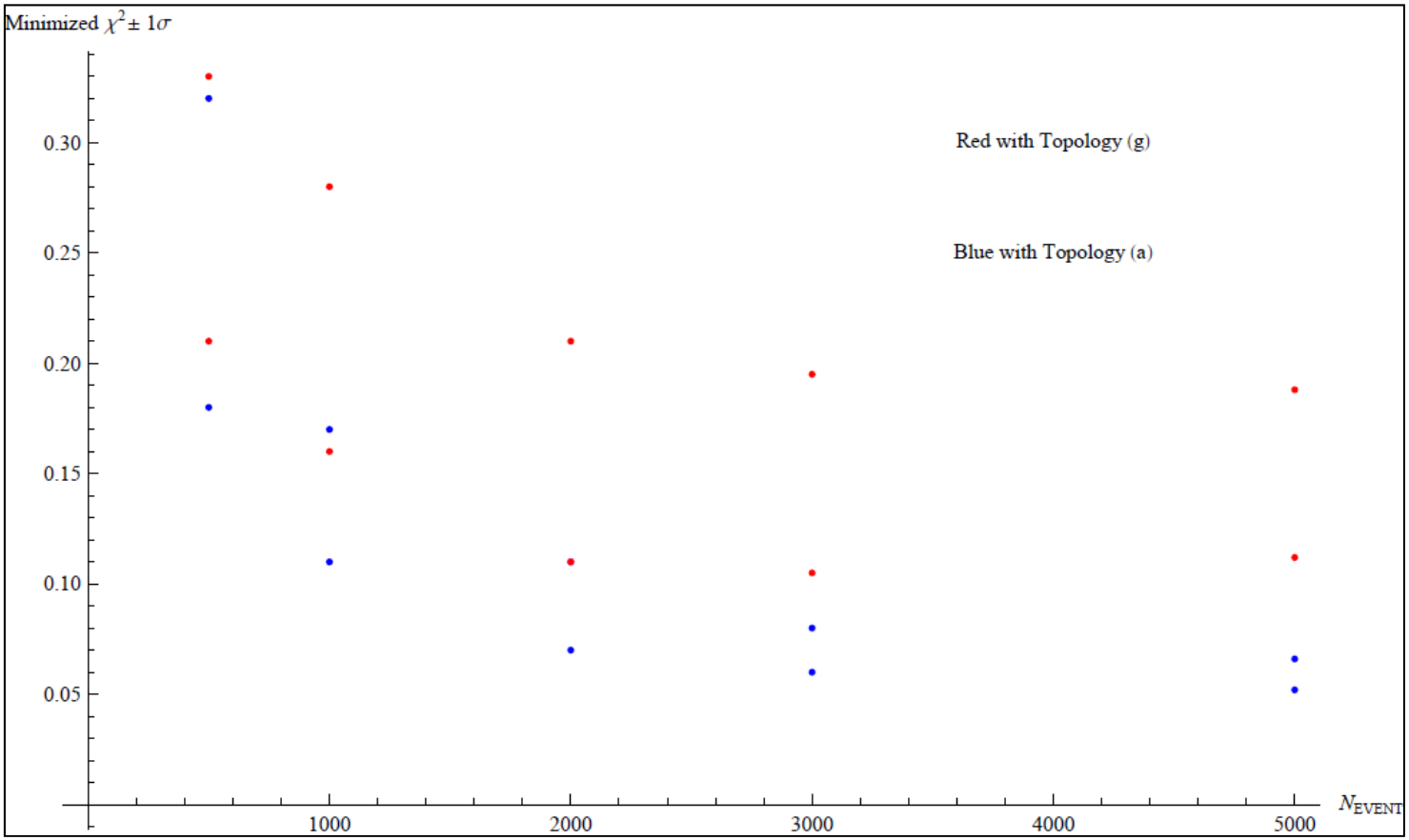

→ 1σ standard error bands of the minimized-χ^2 of a pair of adjacent topology (a) and (g), w.r.t the reference distribution. (very preliminary)

→ Obtained from 2000 experiments

→ Looks to have discrimination power with N_{EVENT} ~O(1000)

Summary

- The robotic arms always have linear shape in their initial lower ranges of the distributions, eventually, showing cusp peak structure.

- The number of rubber arms in a given topology makes their initial distributions apart from the linear, and this provides good measure for the discrimination from the pure robotics, regardless of the mass spectrums.

- Each topology is populated in the unique and well-separated region on the P/E vs R2 plane with strong correlation between the two observables. Then, given a measured peak position, fitting over the (upper peak) region can provide good discrimination power among the rubber arms.

Backup : Aspect of mass measurement using the shape of the rubber arms – Ex) Topology (a), the simplest.

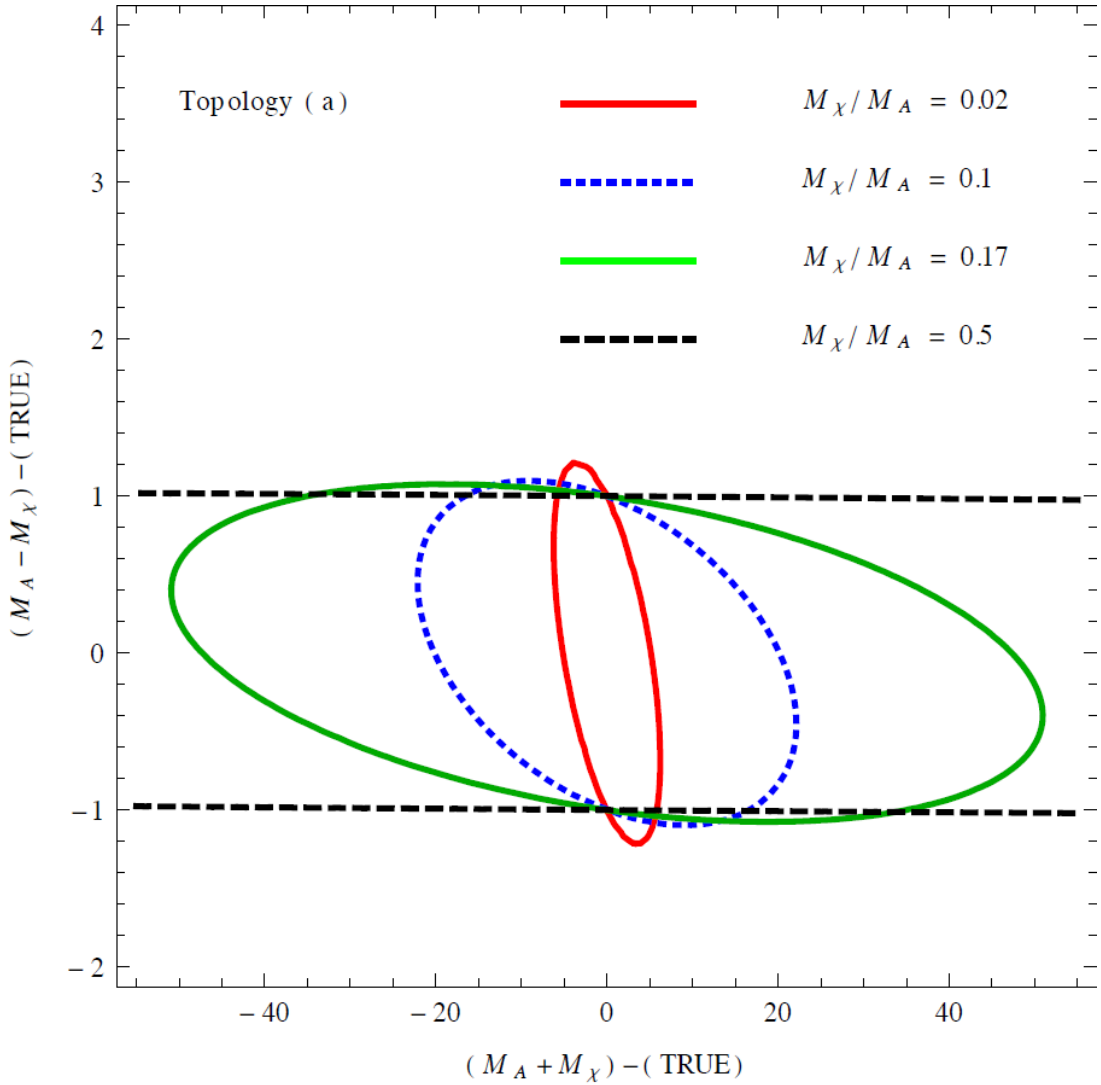

- X^2 - error ellipses on two mass parameter plane from the topology-(a) with various mass spectrums
- In this plot, it is only meaningful to see the ratios of the two errors, σ1 and σ2, each corresponds to the length of the semi-major axis and semi-minor axis.
- In the small mass limit of the DM, the error for mass sum can be as precise as the mass difference, while blowing up in degenerate mass limit.